Marine Technology, Vol. 36, No. 2, April 1999, pp. 112–125

Features of the Wakes of Partly Immersed Wheels

Keith Alexander[1,2]

ABSTRACT

The wakes of partly immersed wheels and paddlewheels are described. The wave trains are compared with boat wakes and are classified into displacement, transition and planing types. The effects that these wake forms can have on a wheel that is being used as a propulsion device are discussed. A significant feature of wheels at high rotational speeds is the stern fountain. Its formation and effects are discussed. Another feature is the overwhelming bow wave which is sometimes present at planing speeds. This is described and factors contributing to its formation are discussed. The control of this bow wave is noted as important particularly for high-speed paddlewheels since its presence limits the speed of operation. It is concluded that these wake features need to be taken into consideration in the design of wheel type propulsion devices. This study is part of a project that developed a type of paddlewheel that supports a load dynamically as it travels at speed over the water surface.

Nomenclature:

D = wheel diameter
F_D = diametral Froude number
F_L = waterline length Froude number
g = gravitational acceleration
h = wheel immersion
L = waterline length
n = revolutions per second
V_a = speed of advance
V_t = wheel rim velocity relative to its axis
θ = immersion angle (see Fig. 1)
$\varnothing$ = blade angle (see Fig. 1)

During the development of an amphibious vehicle, the Lifting Paddlewheel Craft (Alexander 1983), it was found that the wakes of the wheels significantly affected their performance as propulsion devices. Reference to earlier studies on paddlewheels used as propulsion devices (Volpich & Bridge 1955, and Wray & Starrett 1970) suggested that these wake effects were not well understood. Some authors were at a loss to explain why their measured propulsion forces reduced dramatically at certain speeds. The wake effects identified in this paper are able to explain these problems. Since new craft concepts involving the

[1] Manuscript received at SNAME headquarters 6 June 1997
[2] Department of Mechanical Engineering, University of Canterbury, Christchurch, New Zealand

operation of wheels over water continue to appear from time to time it is of some value to describe the wake features that were identified in the Lifting Paddlewheel project. (The Lifting Paddlewheel is a bladed wheel which provides a lift as well as propulsive force, Alexander 1983 a,b))

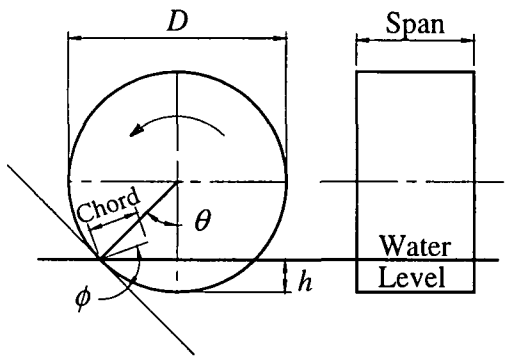

Figure 1: Dimensions of a paddlewheel

While these observations were made initially in relation to work with lifting paddlewheels, they have been found to apply to most types of wheels in water. Other such waterwheels are:

- treaded wheels such as those on all-terrain vehicles
- paddlewheels used solely for low speed propulsion (F_L < 0.85) such as those of Volpich & Bridge 1955
- paddlewheels used for high-speed propulsion (F_L < 0.85) such as used by Beardsley 1973
- wheels used in amphibious vehicle applications (Wray & Starrett 1970, Kearsey 1971)
- smooth cylinders used in a number of attempts at high-speed, over-water transport (Lombardini & Fidderman 1948, Epshteyn 1977).

In order to investigate the case generally, a smooth cylinder, a treaded tire, and a range of bladed paddlewheels were used in this study.

Dimensionless Groups

As with other watercraft, the speed of advance may be defined in dimensionless terms by its waterline length Froude number F_L.

$$F_L = \frac{V_o}{\sqrt{gL}}$$

In the case of a wheel the waterline length L is difficult to measure, so it may be more convenient to redefine L in terms of the wheel immersion h so that the waterline length Froude number becomes:

$$F_L = \frac{V_o}{\sqrt{2g(h(D-h))^{1/2}}}$$

For wheels, an alternative Froude number may be based on the wheel diameter, denoted the diametral Froude number, F_D. The waterline length Froude number F_L, may be related to the diametral Froude number F_D, by:

$$F_L = \frac{F_D}{\sqrt{\sin\theta}}$$

The speed of rotation, and speed of advance can be given in a dimensionless form as the velocity ratio:

$$\frac{V_o}{V_t}$$

and the speed of rotation is given by a rotational Froude number:

$$\frac{nD}{\sqrt{gD}}$$

The immersion of a wheel may be defined as the dimensionless ratio:

$$\frac{h}{D}$$

Wave Train of a Partly-Immersed Wheel Moving in Water

Wheel wave trains, like ship wave trains, may be described in terms of the dispersive theory of waves in deep water (described for example by Lighthill 1979). In this theory the form of the wave train is dependent upon the speed of advance of the moving object, and the speed the waves travel depends on their wavelength.

It has been found useful when considering wheels, to classify the wave formation into three main types,

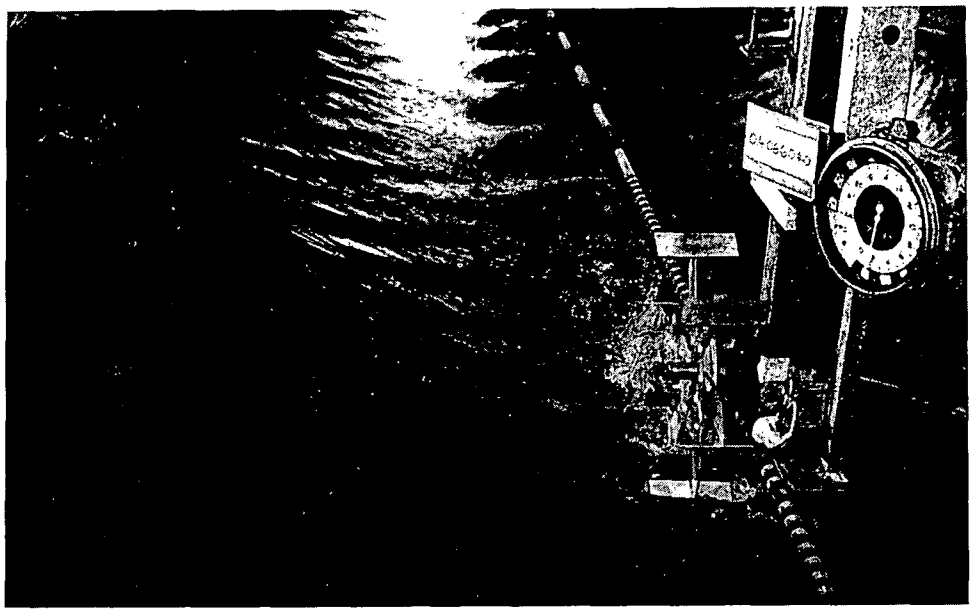

Figure 2: Paddlewheel in the displacement mode showing the short wavelength wave train. $F_L = 0.30$, $nD/\sqrt{gD} = 0.28$, $V_d/V_t = 0.29$, $h/D = 0.17$, $s/D = 0.31$, $c/D = 0.10$

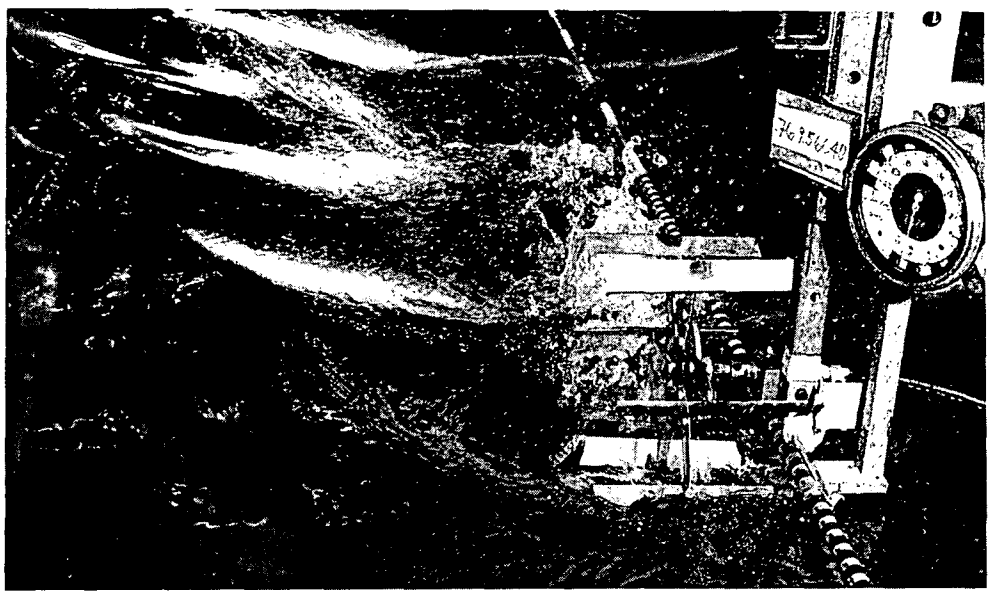

Figure 3: Paddlewheel in the transition mode showing the large amplitude transverse wave train, and the wheel in the wave trough. At higher revs than this the trough is completely scooped out. $F_L = 0.57$, $nD/\sqrt{gD} = 0.31$, $V_d/V_t = 0.5$, $h/D = 0.17$, $s/D = 0.63$, $c/D = 0.10$

Figure 4: Paddlewheel in the planing mode showing without bow splash. F_L=78, $nD/\sqrt{gD}$ = 0.63, $V_j/V_t = 0.78$, $h/D = 0.17$, $s/D = 0.63$, $c/D = 0.10$

Figure 5: Paddlewheel in the planing mode showing substantial bow splash. F_L= 1.78, $nD/\sqrt{gD}$ = 1.1, $V_j/V_t = 0.56$, $h/D = 0.17$, $s/D = 0.63$, $c/D = 0.10$

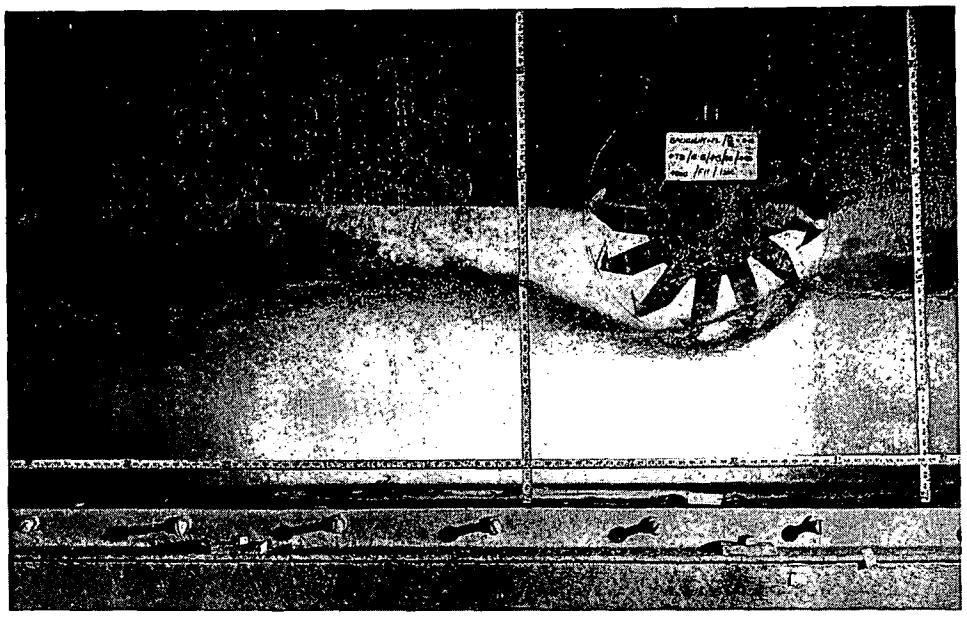

Figure 6: Paddlewheel in the late transition mode showing the large amplitude transverse waves in the glass-sided flume. Flow is from right to left. $F_L = 0.59$, $nD/\sqrt{gD} = 1.0$, $V_i/V_t = 0.16$, $h/D = 0.17$, $s/D = 0.31$, $c/D = 0.10$

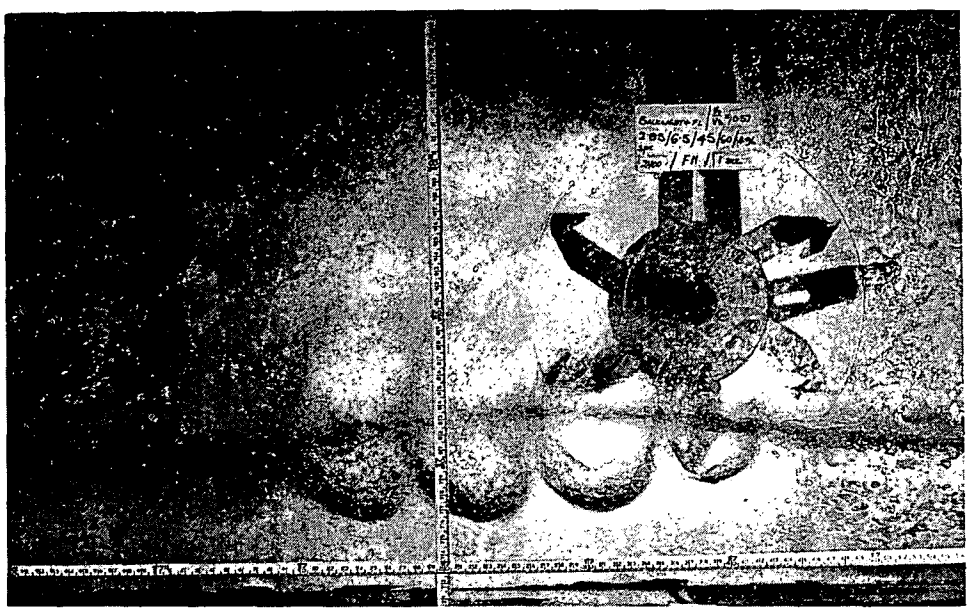

Figure 7: Paddlewheel in the planing mode showing cavities left by the blades. Flow is from the right to left in the glass-sided flume. $F_L = 2.1$, $nD/\sqrt{gD} = 1.0$, $V_i/V_t = 0.56$, $h/D = 0.21$, $s/D = 0.31$, $c/D = 0.10$

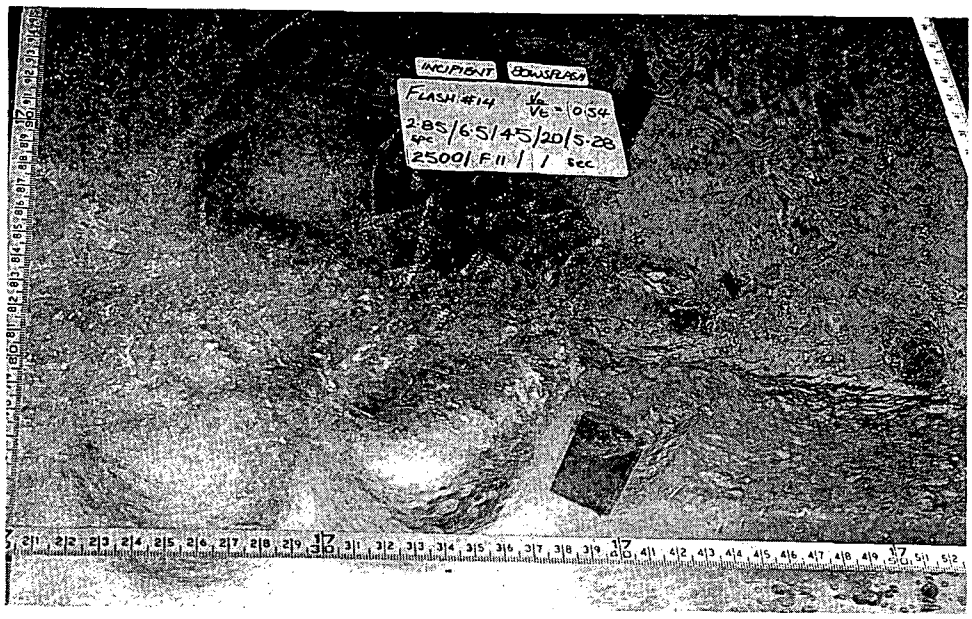

Figure 8(a): Looking up from below at the wheel in Figure 7. Flow is from the right to left. F_L= 2.2, $nD/\sqrt{gD}$ = 1.1, V_j/V_t = 0.54, h/D = 0.17, s/D = 0.31, c/D = 0.10

Figure 8(b): Bow splash now beginning to build with slightly increased rps. Compare the gap between the cavity leading edge and the blade aft edge in this figure and 8(a). F_L= 2.2, $nD/\sqrt{gD}$ = 1.11, V_j/V_t = 0.53, h/D = 0.17, s/D = 0.31, c/D = 0.10

depending on the speed of advance. This is sometimes done for other watercraft:

1. Displacement, where:	$F_L < 0.6$
2. Transition:	$0.6 < F_L < 0.85$
3. Planing:	$F_L > 0.85$

At low speeds of advance, ($F_L < 0.6$) when the wheel is creating the displacement type wake, the wavelength of the waves which are travelling at the speed of the wheel is sufficiently small that wave peaks may appear along the sides of the wheel. These cannot usually be seen with a bladed wheel, as blade impacts tend to disturb them (Figure 2). They may be seen more readily on unbladed wheels such as the smooth cylinder shown in Figure 11. At these low speeds of advance the wave train has little effect upon wheel performance.

For bladed wheels used for propulsion, the water mass supply to the blades is through the sides and bottom of the cavity scraped out by the blades as described by Beardsley (1973). Forces are generated throughout the cavity wherever the blades encounter water.

As the speed of advance is increased to $F_L \sim 0.6$ the waves travelling with the wheel increase in wavelength until a situation is reached where the wheel sits in the trough of the wave travelling with it. In this condition the rear edge of a rotating wheel tends to accentuate the height of the stern wave peak so that both the wheel shape itself, as well as the wheel rotation reinforce the wave formation. As a result large amplitude transverse waves are produced and the wheel sits in a wave trough of approximately the same curvature as the wheel itself. In this condition water mass supply to the wheel can be very limited; the blades of a propulsion paddlewheel have very little engagement with the water in the cavity, with the result that only small forces can be generated, even though the wheel may be rotated very fast. Volpich & Bridge (1955) noted this loss of propulsive force though they did not mention the waveform as its reason.

As the speed of advance is further increased through the transition zone, (where $F_L \sim 0.6$ to $F_L \sim 0.85$), the wavelength of the wave travelling with the wheel becomes longer. The wheel begins to leave its stern wave peak behind and cut into its bow wave. This is shown for a bladed wheel in Figures 3 and 6. The wave amplitudes decrease, as they are no longer being reinforced by the wheel shape and wheel rotation. The mass inflow to the wheel comes increasingly from ahead, so that forces are generated only in the forward part of the cavity made by the wheel.

As the speed of advance progresses into the planing region, where $F_L > 0.85$, the wavelength of the transverse waves becomes much longer and their amplitude becomes relatively insignificant. The wave train of the wheel is now seen to be composed of the small amplitude oblique waves characteristic of planing craft; these are barely visible in Figure 4 of the bladed wheel, but more notable in Figure 13 for the smooth cylinder. Now the mass inflow to the wheel is completely from ahead. For the bladed wheel the generation of forces is found to occur, to a working approximation, at the point where the blade enters the water (Alexander 1983 (a)).

Further increases in the speed of advance make no significant changes to the waveform at the wheel.

Overwhelming Bow Wave at Planing Speeds

If a bladed wheel is moving at a given planing speed ($F_L > 0.85$) it will be observed that there are two conditions of operation which depend primarily upon the wheel's speed of rotation, V_t. At a low speed of rotation ($V_a / V_t \sim 0.84$), no bow splash is present as shown in Figure 4, but at a higher speed of rotation ($V_a / V_t \sim 0.43$), the wheel produces a substantial frothing bow splash as shown in Figure 5. Under conditions described below this may build up and swamp the wheel. Significantly this bow splash is entirely absent below planing speeds, irrespective of the speed of rotation.

Because this bow splash can overwhelm and submerge the wheel, it must be avoided for high-speed operation of paddlewheels. And when it can be prevented it allows the paddlewheel to be operated to unlimited speeds of advance. Because of its importance for the high-speed operation of paddlewheels some attempts have been made to determine the velocity ratio, $\frac{V_a}{V_t}$ at which this bow splash begins to occur. Several features of the phenomenon have been isolated:

1. Observations of paddlewheels in operation such as shown in Figure 7, have suggested that the bow splash begins to build up when each descending blade is just about to enter the cavity left in the water by the previous blade. In this situation the descending blade encounters the splash from the forward edge of the cavity left by the previous blade.
2. Analytical predictions based on this idea have been acceptably consistent with the observations, but only for the variables of: number of blades, wheel immersion, blade angle $\varnothing$, and blade chord.

3. The analysis, however, has always predicted the bow splash to occur at too high a rotational speed, V_t. Closer observation has shown the bow splash to begin to build at a somewhat lower rotational speed, just before the descending blade breaks into the cavity left by the previous blade. A satisfactory empirical adjustment has been to assume that bow splash begins to occur when the inside edge of the descending blade is half a blade chord ahead of the previous cavity edge. This can be seen to be case in Figures 8(a) on the point of producing a bow splash and 8(b) where bow splash is just building up.
4. The forces generated by planing bladed wheels differ in character before and after the onset of the bow splash. An example of this change in force is shown in Fig. 9 from the Lifting Paddlewheel project. The reason for this change in force is not the bow splash as such, but the fact that each descending blade is now breaking into the cavity left by the last blade.

Bow splash for paddlewheels can be avoided then, by arranging for the immersion depth and velocity ratio to be such that the descending blade is at least half a blade chord ahead of the cavity left by the previous blade. In practical terms this usually means keeping the wheel rotational speed down, and not letting the wheel sink too deeply.

Wake Features of a Smooth Cylinder Compared with a Bladed Wheel

In the present series of tests it was found that the wake of a cylinder while similar in most respects to the wakes of bladed wheels, had some notable differences:

Wave Trains

The cylinder wave train was essentially similar to that of the paddlewheel for the lower speed regimes. This can be seen by comparing the cylinder in Figure 11 with the paddlewheel in Figure 2, where the displacement type wakes are shown in both cases. Similarly the cylinder in Figure 12 and the paddlewheel in Figure 3 show transition type wakes with the pronounced transverse waves.

At planing speeds the wakes begin to show differences. The oblique wave trains of a planing type wake are still present for the cylinder in Figures 13 and 15. These are to be compared with Figures 4 and 5 for the paddlewheel, where the oblique wave trains are difficult to see in the photographs, being all but obscured by spray.

But while the wave trains remain comparable between the smooth cylinder and the bladed wheel, there are major differences in the bow wave and the stern fountain.

Bow Wave in a Smooth Cylinder

At planing speeds (F_L > 0.85) the cylinder produced a bow wave irrespective of its speed of rotation. This is shown in Figure 13 where there is no rotation and Figure 15 with a high rotational speed. These are to be compared with the paddlewheel where in Figure 4 at a low speed of rotation there is no bow splash, while in Figure 5 at a higher speed of rotation there is a significant bow splash.

Smooth cylinders have been examined by Epshteyn (1977) where he considered only planing operation (F_L >4). He showed that for a cylinder the bow wave is equivalent to the frontal spray jet thrown forward by a planing surface.

This suggests how a paddlewheel bow splash may be viewed. As a paddlewheel increases its revolutions it presents more nearly a cylindrical surface towards the incoming flow from ahead, and at some point it begins to behave like a continuous cylinder producing a bow wave. This "bow wave" of the bladed wheel, however, is really composed of the individual splashes thrown forward as each successive blade enters the water. These merge into a boiling wave very similar to the frontal spray jet thrown forward by a planing surface.

It is significant that the bow splash in a bladed wheel only occurs at planing speeds and not at displacement or transition speeds. This indicates that it is a gravitational effect.

A similar bow wave form has been sketched and acknowledged in studies of cylinders and spheres in ricochet from a water surface (Hutchings 1976, Miloh & Shukron 1991). These studies suggest that the bow wave will tend to submerge the cylinder once the cylinder center is below the waterline.

Stern Fountain

In Figure 14 at transition speed and Figure 15 at planing speed the rotating cylinder produced a stern fountain. This fountain occurred at all speeds of advance for the cylinder. At low speeds of advance the fountain piles up over the wheel as in Figure 14, while at the planing speed in Figure 15 the fountain is much more spread out by the wheel's forward motion.

By contrast the bladed wheel at planing speed in Figure 5, has only a scattering of spray above the wheel. The stern fountain is almost entirely absent. Most of the spray is in a horizontal wake out behind it.

During the Lifting Paddlewheel experiments it was found that wheels with an especially high density of blades could produce a stern fountain similar to that of

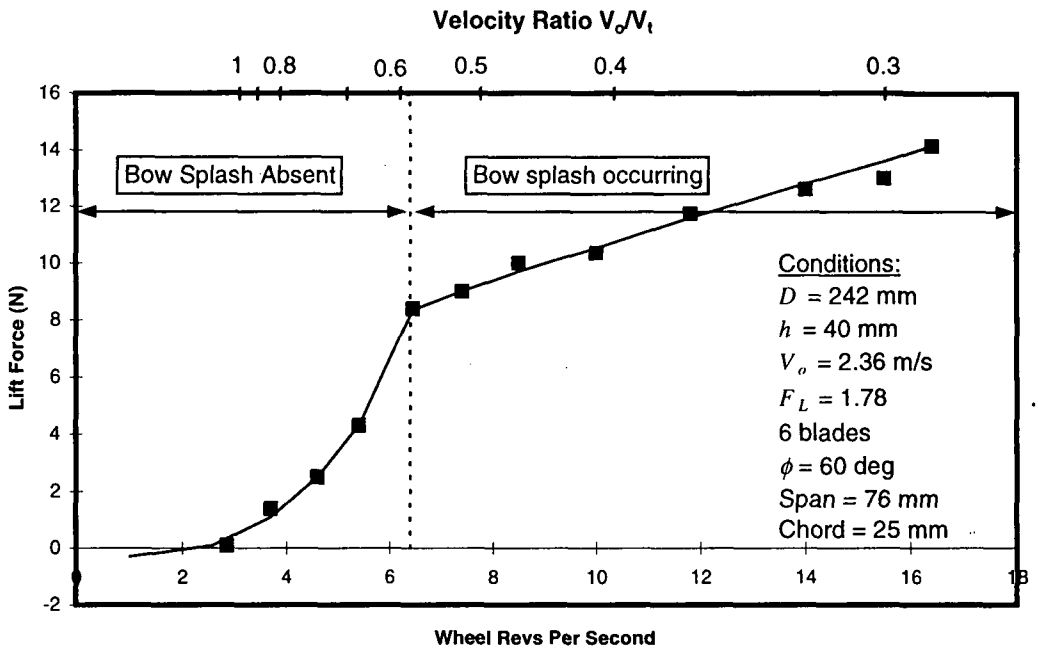

Figure 9: The force-RPS plot for a lifting paddlewheel in the planing mode, showing the change in force before and after bow splash.

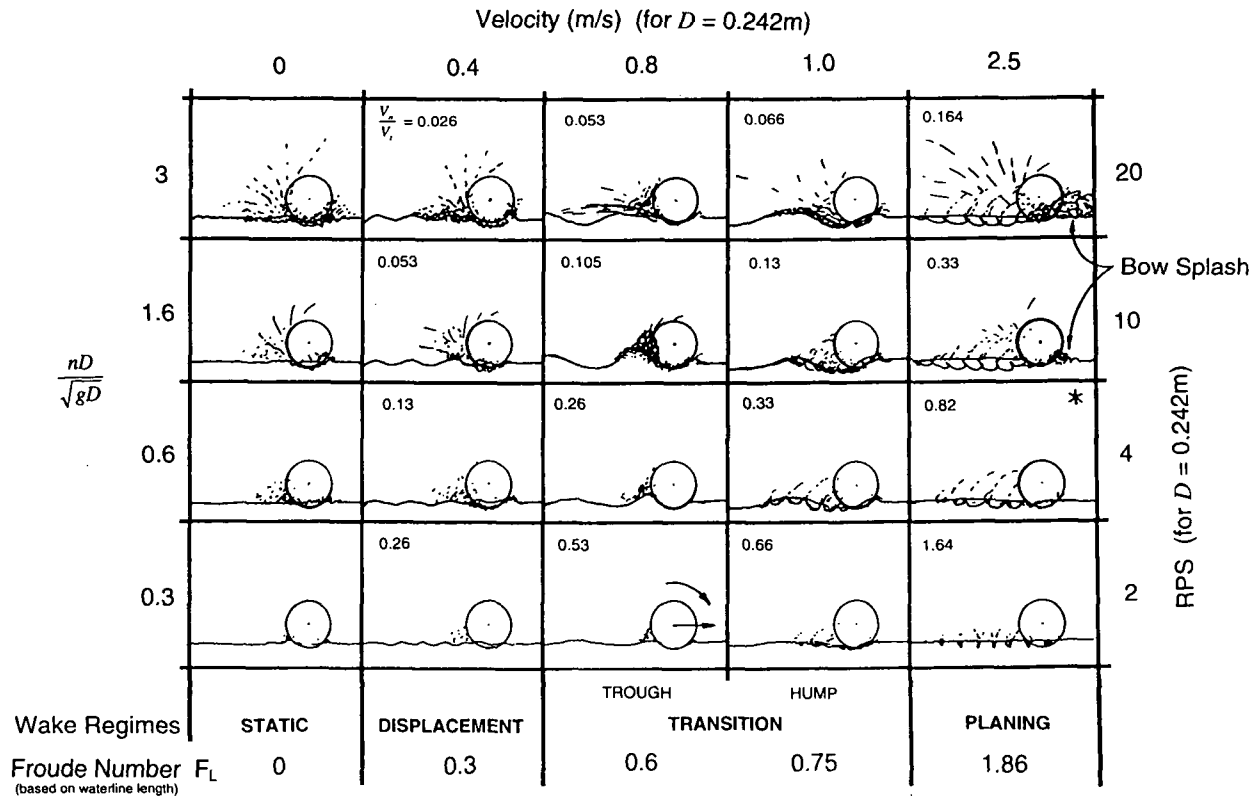

Figure 10: Sketches of the wake formations for paddlewheels (h/D = 0.15, 6 blades) (* Effective Operation)

the smooth cylinder. In fact at low speeds of advance, and high rotational speeds some of these paddlewheels produced a massive stern fountain which drove the experimental craft below the water rather than lifting it up on to the water surface. Whether or not this stern fountain occurred was critical for the operation of that craft.

From these observations it seems that the mass of water in this fountain depends in part upon its speed of rotation, V_t, and in part on the area and nature of the rotating surface. With the smooth cylinder the water pickup is believed to be primarily a boundary layer effect. With bladed wheels or tires (Figure 16) the pickup appears to be a combination of boundary layer and the flow becoming trapped between the blades. It is therefore largely absent in the bladed paddlewheels with large spaces between the blades, such as in Figure 5.

Tests with Treaded Tires

Tests with treaded tires were in most respects similar to the tests with the smooth cylinder. Figure16 shows a treaded tire at planing speed. It produced the same wave trains, and at planing speeds a bow wave at all speeds of rotation, much like the smooth cylinder. It also produced a significant stern fountain which was a little more broken up than that of the smooth cylinder.

The Integrated Picture

Figure 10 shows in sketch form, the range of wakes for paddlewheels with well-spaced blades. On the horizontal axis the speed of advance increases through the wake stages to planing. On the vertical axis the rotational velocity is increased from too slow for propulsion, to excessive. The observed wake features are pointed out. Notably absent is the stern fountain, because this would not be present in most paddlewheels designed for propulsion. Included are actual values for the experimental test wheel, as well as the dimensionless numbers defining the velocities. In each box is the velocity ratio. It is intended that this chart can readily show the wake features as well as making it easy to determine the features to be expected for given set of paddlewheel velocity conditions.

A Note on Observations in Flumes of Flowing Water

Figures 6, 7, 8(a) and 8(b) are stroboscopic studies of the paddlewheel in a flume of flowing water. While they demonstrate the phenomena described above as occurring at approximately the right open-water velocities, they have limited validity. This is because:

(a) the sides of the flume constrain the flow in one dimension, and
(b) shallow flowing water in open channel flow will produce its own wave formations without any paddlewheel present.

Strictly speaking, what is observed in these figures is a combination of the effects of the paddlewheel and the flume flow phenomena. However, with this in mind it has been helpful to use the flume to clarify flow features that are more difficult to observe (and to photograph) in open-water tests.

As an example of this, the rise of the surface in Figure 7, where the flow passes the paddlewheel is only observable in the flume. This is a continuity effect caused by the glass walls and floor of the flume, which do not allow room for expansion of the flow when a blade cavity is present. This surface rise is not observed in open water.

Concluding Remarks

While a lone wheel moving through the water will produce the wake features described above, a wheel is rarely isolated in practice. It will almost always be mounted on some waterborne craft with a wake of its own. In such a case it is the combination of the wakes of the wheel and the supporting craft, which will affect the performance of the wheel. Some designers, such as Volpich & Bridge 1957, have found that wheel performance under certain operating conditions can be dramatically reduced by the presence of a hull wave train.

Others have taken advantage of the wake features of the supporting hull and have placed wheels in carefully chosen positions such as behind the transom of a planing craft (Wray & Starrett 1970). In this case the inflowing water mass to the paddlewheel was at a controlled height and with a horizontal flow direction.

The significant points are that for wheels or paddlewheels to act as propulsion devices they need an appropriate mass supply which is not depleted by the wake of the supporting craft. And they need to be

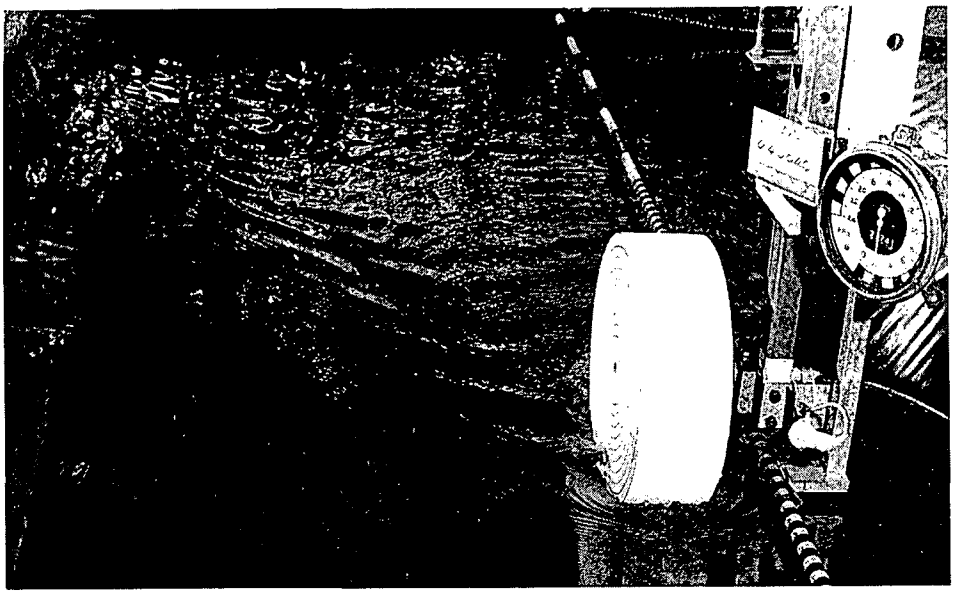

Figure 11: The smooth cylinder in the displacement mode showing the short wavelength wave train. F_L=0.30, $nD/\sqrt{gD} = 0$, $V_t/V_t = 0$, $h/D = 0.17$, $s/D = 0.31$

Figure 12: The smooth cylinder in the transition mode at low rps, showing large amplitude transverse waves. F_L= 0.57, $nD/\sqrt{gD} = 0.39$, $V_t/V_t = 0.4$, $h/D = 0.17$, $s/D = 0.31$

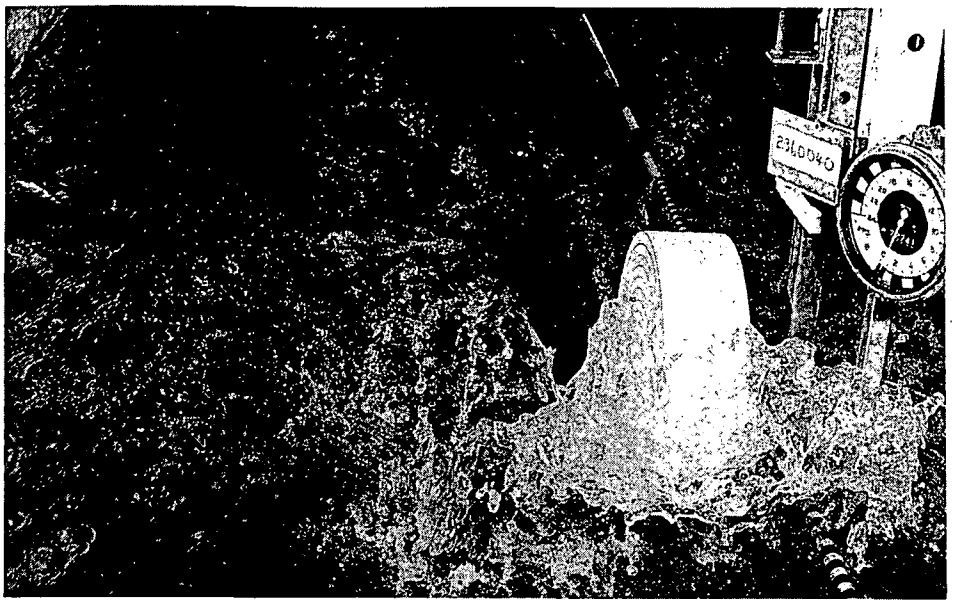

Figure 13: The smooth cylinder in the planing mode at zero rps, showing large bow splash.
$F_L = 1.78,\ nD/\sqrt{gD} = 0,\ h/D = 0.17,\ s/D = 0.31$

Figure 14: The smooth cylinder in the transition mode at high rps, showing a large stern fountain.
$F_L = 0.57,\ nD/\sqrt{gD} = 2.2,\ V_i/V_t = 0.07,\ h/D = 0.17,\ s/D = 0.31$

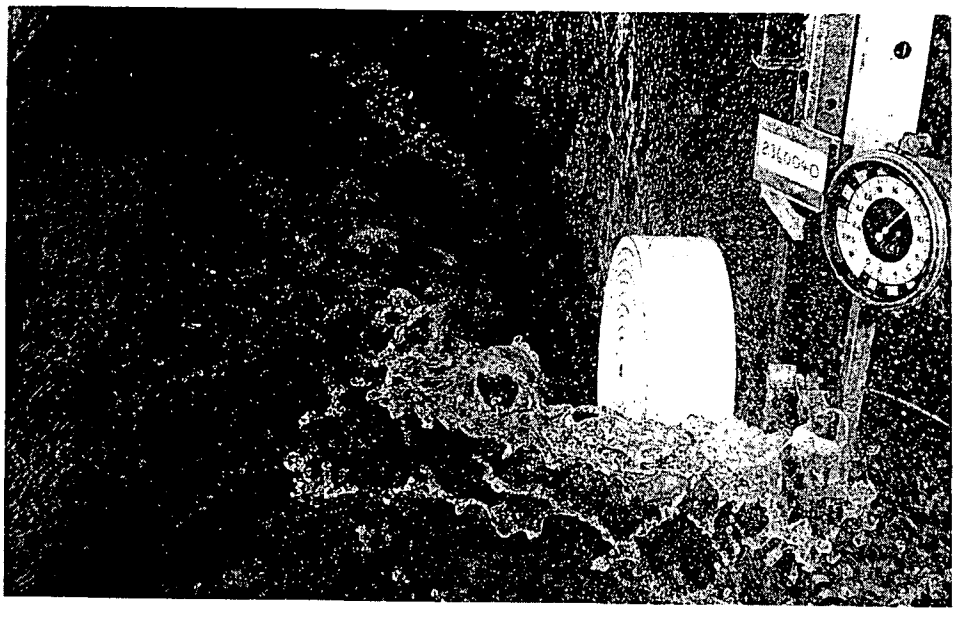

Figure 15: The smooth cylinder in the planing mode at high rps, showing reduced bow splash and stern fountain. F_L= 1.78, $nD/\sqrt{gD}$ = 2.1, V_a/V_t = 0.23, h/D = 0.17, s/D = 0.31

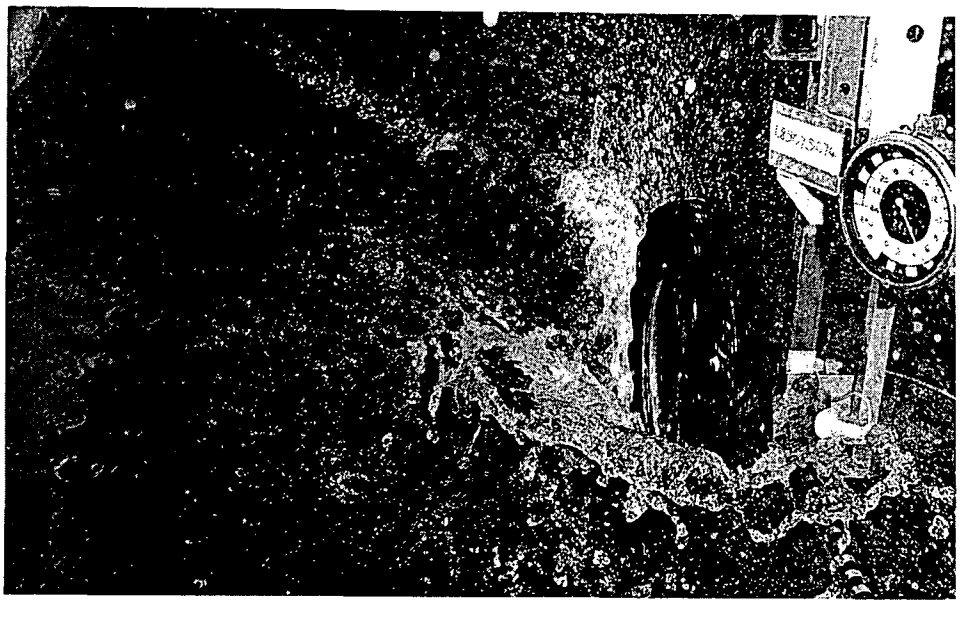

Figure 16: The treaded tire at planing speed showing the oblique wave train, bow wave and a broken stern fountain. F_L= 1.15, $nD/\sqrt{gD}$ = 0.87, V_a/V_t = 0.4, h/D = 0.3, s/D = 0.25, c/D = 0.03, 30 blades

designed and operated in such a way as to avoid the worst effects of the bow wave and the stern fountain.

For any craft operating with wheels over water it is important to have these wake effects taken into account because, as has been shown, the wake effects can completely alter the forces expected from the wheels.

REFERENCES

Alexander, K. V. "The Lifting Paddlewheel, a non-buoyant wheel enabling a high-speed wheeled craft to run on the water surface," Doctoral thesis, University of Canterbury, New Zealand 1983.

Alexander, K.V. "Prototype Model Tests of a High-speed Wheeled Amphibious Vehicle" *Proceedings, 8th Australasian Fluid Mechanics Conference, Newcastle NSW*, Vol. 1, 4C.10, 1983.

Beardsley, M.W. "Surface Impulse Propulsion: a review and comment on future potential." *Hovercraft & Hydrofoil*, Vol. 12 No. 9, June 1973, pp. 10-24.

Hutchings, I.M. "The Ricochet of Spheres and Cylinders from the Surface of Water," *International Journal of Mechanical Engineering Science*, Vol 18, 1976, pp. 243-247.

Kearsey, J.A. "The Rollercraft, "*Hovercraft and Hydrofoil*, Vol. 10, No. 12, Sept 1971, pp.14-25.

Lighthill, M.J. *Waves in Fluids*, Cambridge University Press, U.K., 1979.

Miloh, T. & Shukron, Y. "Ricochet off Water of Spherical Projectiles," *Journal of Ship Research*, Vol. 35, No. 2, June 1991, pp. 91-100.

Volpich, H. & Bridge, I.C. "Paddlewheels, Pt 1: Preliminary Model Experiments," Paper No. 1193, *Transactions of the Institution of Shipbuilders and Engineers of Scotland*, Vol. 98, Feb. 1955, pp. 327-380.

Volpich, H. & Bridge, I.C. "Paddlewheels, Pt 2: Systematic Model Experiments," Paper No. 1208, *Transactions of the Institution of Shipbuilders and Engineers of Scotland*, Vol. 99, March 1956, pp. 467-510.

Volpich, H. & Bridge, I.C. "Paddlewheels, Pt 2a: Further Model Experiments. Pt 3: Ship/Model Correlation," Paper No. 1222, *Transactions of the Institution of Shipbuilders and Engineers of Scotland*, Vol. 100, Feb 1957, pp. 505-550.

Wray, G. A. & Starrett, J. A. "A model study of paddlewheel propulsive devices for high-speed craft," Davidson Laboratory, Stevens Institute of Technology, Report No. SIT-DL-70-1428, Hoboken, NJ, 1970.